

## Electronic Supplementary Information (ESI)

Controlled synthesis of open-mouthed epitope-imprinted polymer  
nanocapsules containing a PEGylated nanocore for fluorescence detection  
of the target protein

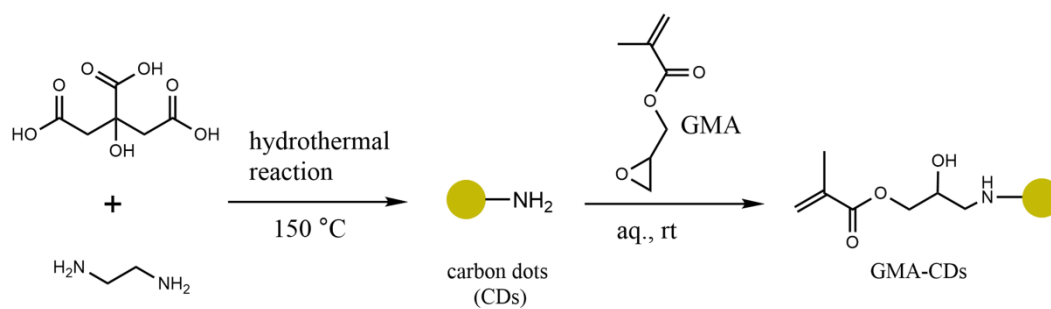
Xingjia Feng, Siyu Jin, Dongru Li, Guoqi Fu\*

Key Laboratory of Functional Polymer Materials of Ministry of Education, Institute of  
Polymer Chemistry, College of Chemistry, Nankai University, Tianjin 300071, China

\* Corresponding author.

E-mail address: gqfu@nankai.edu.cn (G. Fu)

Tel: 86 22 23501443



**Scheme S1.** Schematic illustration of the procedure for the synthesis and subsequent surface functionalization of carbon dots.

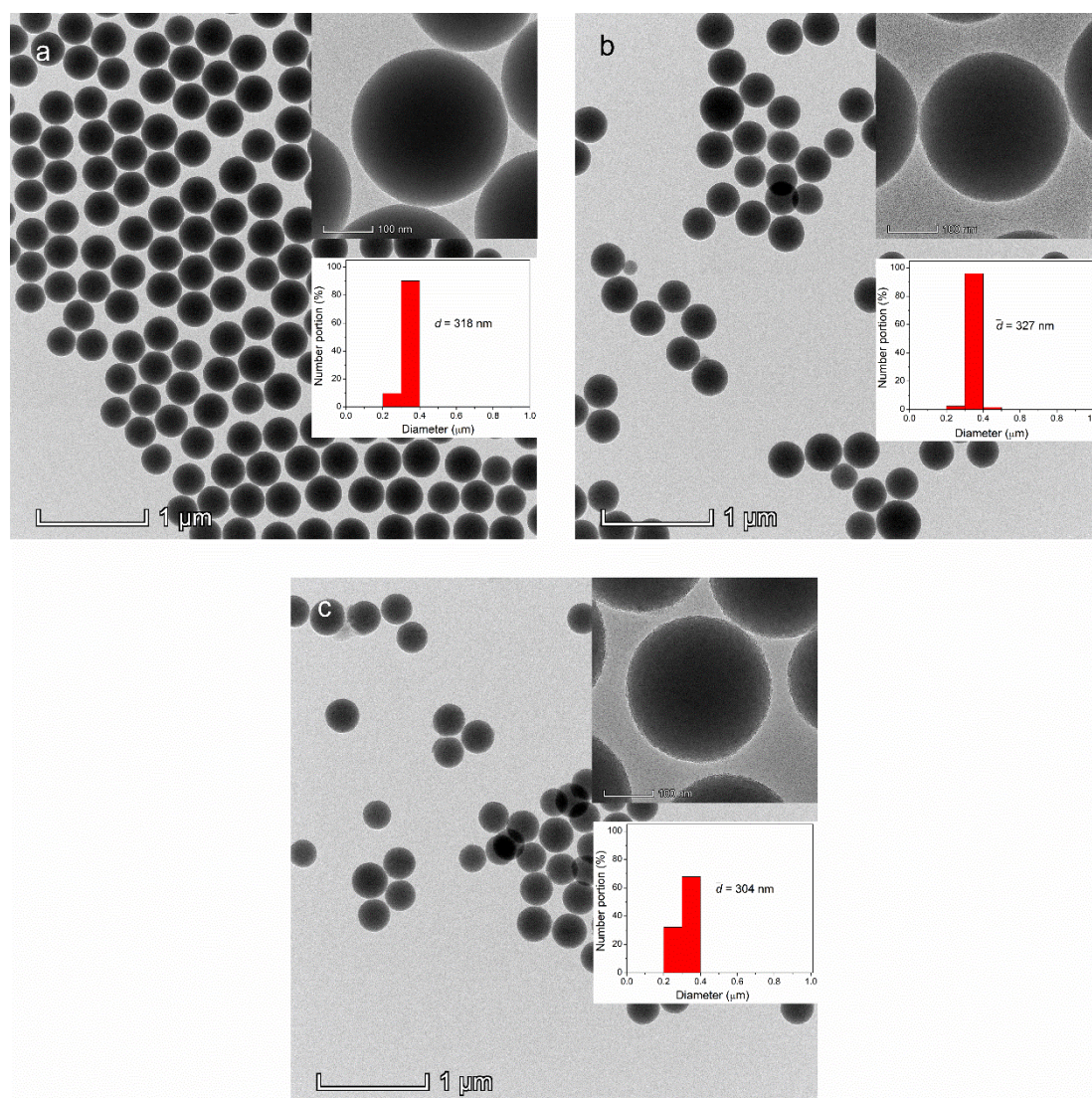


**Fig. S1.** TEM images of (a) the original SiO<sub>2</sub> NPs, (b) MIP JNPs obtained by surface-initiated ATRP over the SiO<sub>2</sub>-NH<sub>2</sub>// epitope/iB-Br JNPs, and (c) OM-MIP NCs obtained after partial

etching the SiO<sub>2</sub> nanocore inside the MIP JNPs. The insets (top) show the high-resolution images with a bar of 100 nm. The insets (bottom) indicate the counted size distribution.

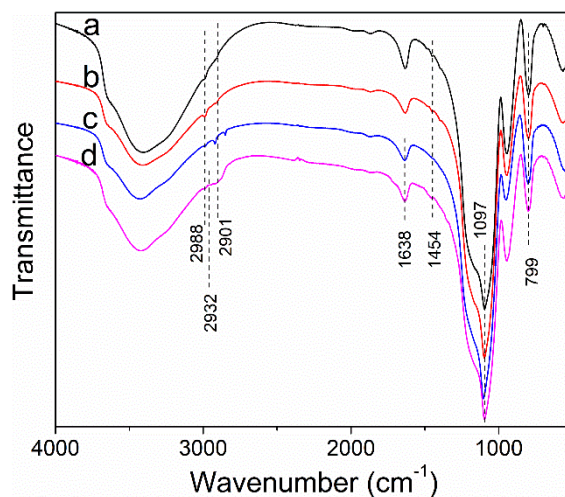


**Fig. S2.** FT-IR spectra of (a) SiO<sub>2</sub> NPs, (b) SiO<sub>2</sub>-NH<sub>2</sub> NPs, (c) SiO<sub>2</sub>-NH<sub>2</sub>//iB-Br/Ac-Br JNPs and (d) SiO<sub>2</sub>-PEG NPs. For all the particles, the strong and broad peak around 1097 cm<sup>-1</sup> indicates the Si-O-Si asymmetric stretching, and the bands observed at around 799 cm<sup>-1</sup> shows the Si-O vibration. For the SiO<sub>2</sub>-NH<sub>2</sub> NPs, the peak at 1454 cm<sup>-1</sup> corresponds to the N-H bending vibration, and the peaks at 2988 cm<sup>-1</sup> and 2901 cm<sup>-1</sup> correspond to the stretching vibration of C-H bonds of the methyl or methylene groups of APTES, confirming the surface modification of SiO<sub>2</sub> NPs by APTES. For the SiO<sub>2</sub>-NH<sub>2</sub>//iB-Br/Ac-Br JNPs, the appearance of characteristic bands at 1638 cm<sup>-1</sup> represents the bromoisobutyrate residue. With respect to SiO<sub>2</sub>-PEG NPs, the two peaks at 2932 cm<sup>-1</sup> and 1638 cm<sup>-1</sup> corresponding to the vibration of -CH<sub>2</sub>- and C=O bonds suggest the successful modification with silanized m-PEG.

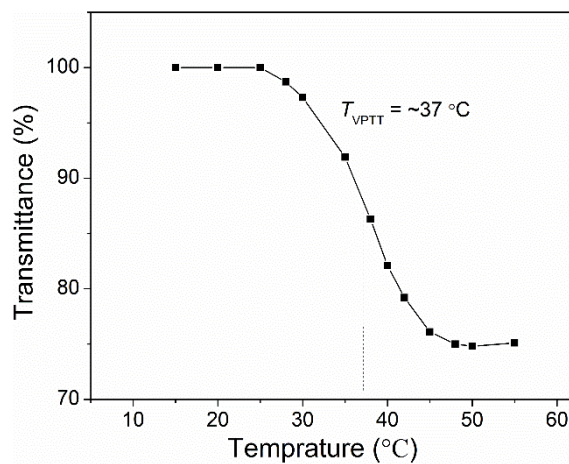


**Fig. S3.** Transmittance of OM-MIP NCs in the PB buffer with increasing temperatures. The volume phase transition temperature (VPTT) was determined to be about 37 °C.

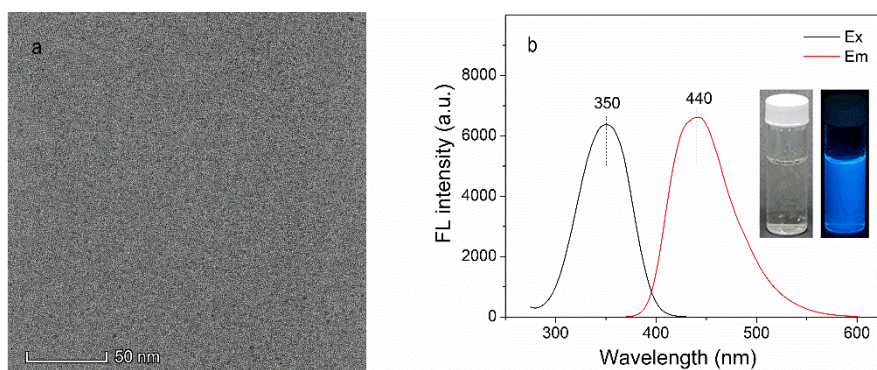


**Fig. S4.** (a) TEM image of the GMA-CDs. (b) FL excitation and emission spectra of the GMA-CDs dispersed in the PB buffer. The insets show the photographs of the GMA-CDs solution under sunlight (left) and a 365 nm UV lamp (right), respectively.

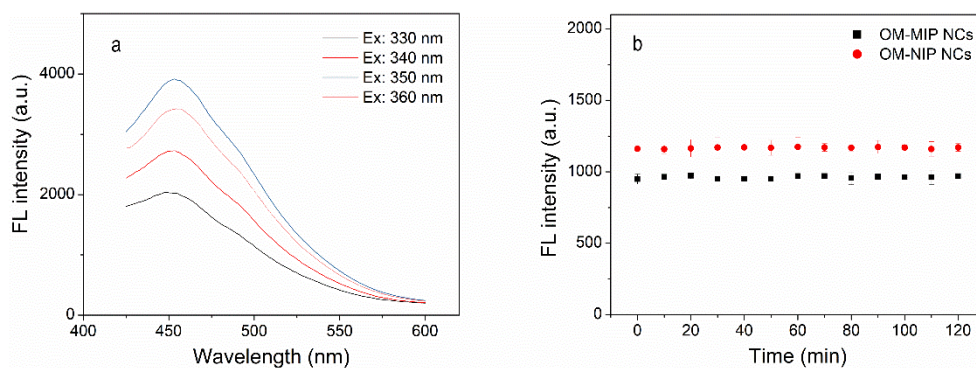


**Fig. S5.** (a) The FL emission spectra of the OM-MIP NCs dispersed in PB buffer under varied  $\lambda_{ex}$ . (b) The FL emission intensity change of the OM-MIP and OM-NIP NCs in PB buffer during continuous FL measurements.

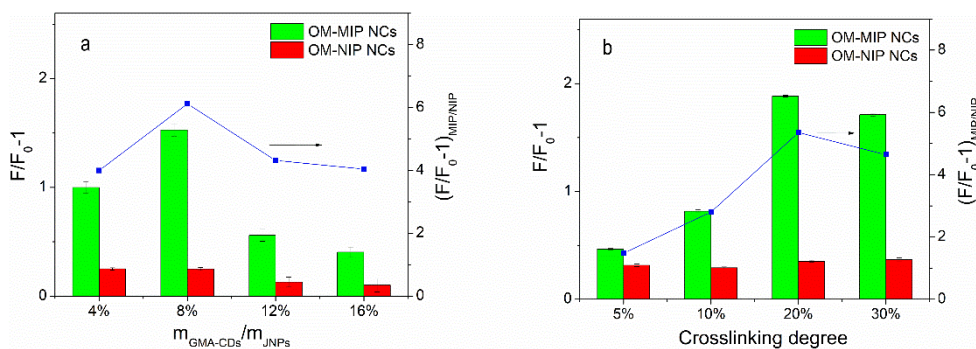


**Fig. S6.** The effect of (a) mass ratio of GMA-CDs relative to support JNPs and (b) molar crosslinking in the polymerization recipe on the FL response of the resultant OM-MIP and OM-NIP NCs.

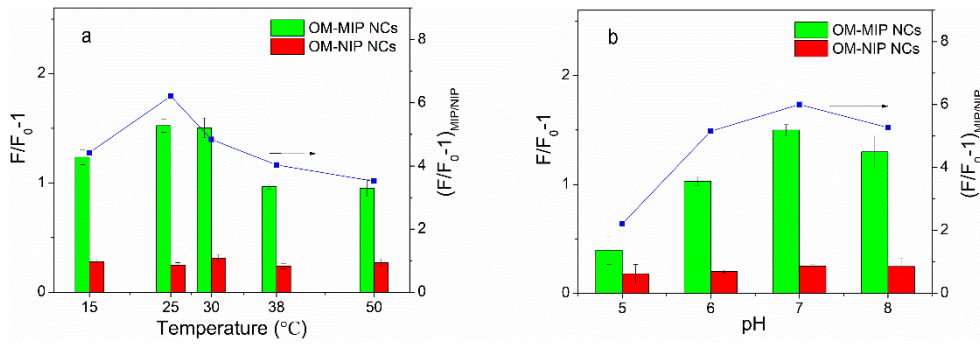


**Fig. S7.** The effect of (a) temperature and (b) pH on the FL response of the OM-MIP and OM-NIP NCs.

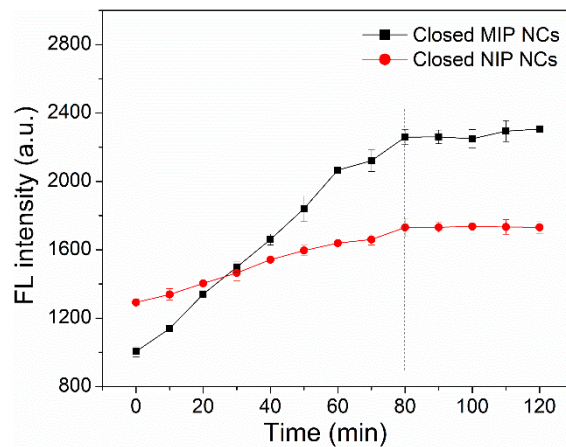


**Fig. S8.** FL response kinetics of the closed MIP and NIP NCs.

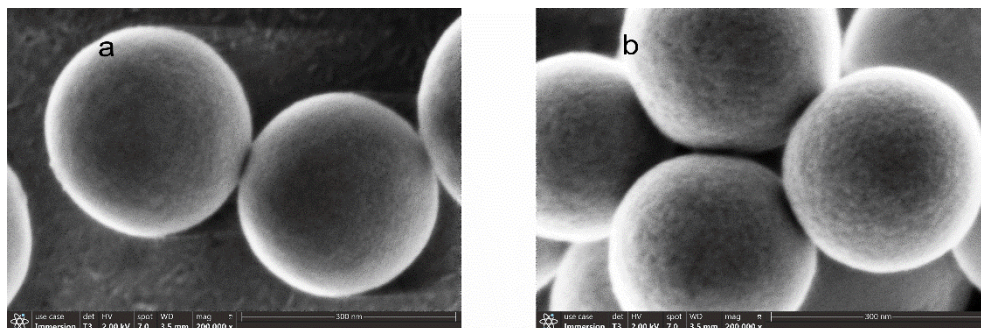


**Fig. S9.** SEM images of (a) the original  $\text{SiO}_2$  NPs and (b) the  $\text{SiO}_2$  NPs after partially etched with 80 mM of  $\text{NH}_4\text{HF}_2$ .

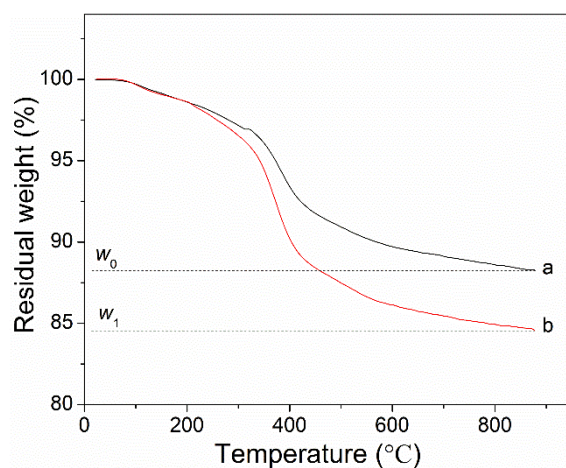


**Fig. S10.** TGA curves of (a) the original SiO<sub>2</sub> NPs and (b) PEGylated SiO<sub>2</sub> NPs. The amount of PEG chains grafted to the PEGylated SiO<sub>2</sub> was estimated to be ~42 mg/g.

**Table S1.** Comparison of the FL detection performance of the reported molecular imprinting based FL sensors for BSA or HSA detection.

FL substance	Template	Linear range (μM)	LOD (nM)	IF <sub>SV</sub>	Ref.
ZnO QDs	BSA	3.0-30	-	2.4	[1]
MWCNT QDs	BSA	0.5-3.5	80.0	4.2	[2]
CdTe/CdS QDs	BSA	2-64	500	1.9	[3]
Dansyl	BSA	0.2-2.65	560	21	[4]
CdTe QDs	C-terminus nonapeptides of HSA	0.25-5	44.3	2.6	[5]
CdTe QDs	C-terminus nonapeptides of BSA	0.5-10	110	4.8	[6]
CDs	C-terminus nonapeptides of BSA	0.2-6	43.8	7.8	[7]
CDs	C-terminus nonapeptides of BSA	0.25-6	38.1	6.1	This work

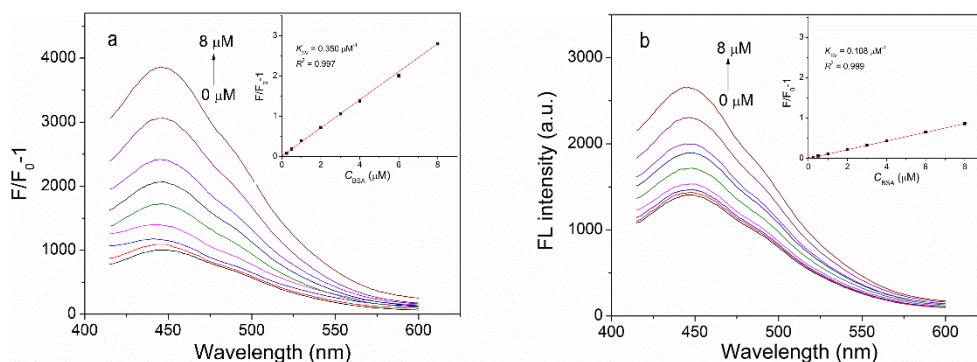


**Fig. S11.** FL emission spectra of (a) non-PEGylated OM-MIP and (b) non-PEGylated OM-NIP NCs in the presence of BSA (0–8  $\mu\text{M}$ ), respectively. The insets show the corresponding Stern–Volmer plots.

**Table S2.** The spiked recoveries and relative standard deviations (RSDs, %;  $n=3$ ) for the detection of BSA in the 1000-fold diluted bovine serum using the OM-MIP NCs.

spiked ( $\mu\text{M}$ )	found ( $\mu\text{M}$ )	recovery $\pm$ RSDs (%) <sup>a</sup>
0	$0.45 \pm 0.02$	-
0.5	$0.97 \pm 0.02$	$104.0 \pm 4.6$
1.0	$1.43 \pm 0.03$	$98.0 \pm 2.6$
2.0	$2.47 \pm 0.03$	$101.0 \pm 1.7$
4.0	$4.44 \pm 0.05$	$99.8 \pm 1.2$

<sup>a</sup> The recoveries were calculated based on the BSA concentration found in the spiked samples after subtraction of that found in the non-spiked sample.



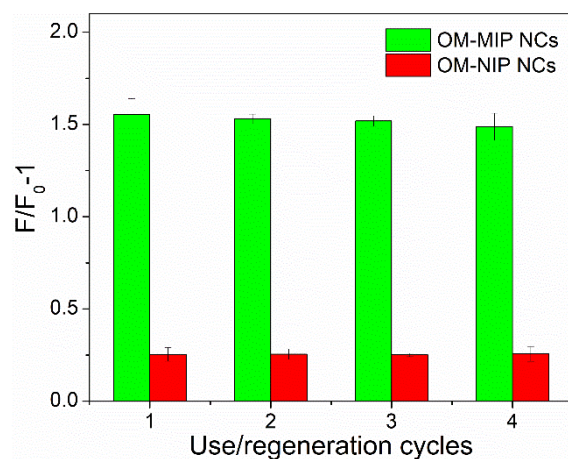


**Fig. S12.** The reusability of the OM-MIP NCs and OM-NIP NCs with 4 use/regeneration cycles. The used NCs were regenerated by washing with 1% SDS/1% acetic acid solution for removal of the BSA bound, followed by washing with NaCl solution (1 M) and water.

## References

- [1] X.J. Li, J.J. Zhou, L. Tian, W. Li, B.L. Zhang, H.P. Zhang, Q.Y. Zhang, Bovine serum albumin surface imprinted polymer fabricated by surface grafting copolymerization on zinc oxide rods and its application for protein recognition, *J. Sep. Sci.* 38 (2015) 3477–3486.
- [2] Z.Q. Ding, S.A. Bligh, L. Tao, J. Quan, H.L. Nie, L.M. Zhu, X. Gong, Molecularly imprinted polymer based on MWCNT-QDs as fluorescent biomimetic sensor for specific recognition of target protein, *Mater. Sci. Eng., C* 48 (2015) 469–479.
- [3] L.S. Wang, L.S. Zhao, A novel nanocomposite optosensing sensor based on porous molecularly imprinted polymer and dual emission quantum dots for visual and high selective detection of bovine serum albumin, *Colloids Surf., A* 632 (2022) 127843.
- [4] E. Battista, P.L. Scognamiglio, N. Di Luise, U. Raucci, G. Donati, N. Rega, P.A. Netti, F. Causa, Turn-on fluorescence detection of protein by molecularly imprinted hydrogels based on supramolecular assembly of peptide multi-functional blocks, *J. Mater. Chem. B* 6 (2018)

1207–1215.

[5] Y.Z. Wang, D.Y. Li, X.W. He, W.Y. Li, Y.K. Zhang, Epitope imprinted polymer nanoparticles containing fluorescent quantum dots for specific recognition of human serum albumin, *Microchim. Acta* 182 (2015) 1465–1472.

[6] Y.Q. Yang, X.W. He, Y.Z. Wang, W.Y. Li, Y.K. Zhang, Epitope imprinted polymer coating CdTe quantum dots for specific recognition and direct fluorescent quantification of the target protein bovine serum albumin, *Biosens. Bioelectron* 54 (2014) 266–272.

[7] S.T. Zhang, Z.Q. Liu, S.Y. Jin, Y.F. Bai, X.J. Feng, G.Q. Fu, A method for synthesis of oriented epitope-imprinted open-mouthed polymer nanocapsules and their use for fluorescent sensing of target protein, *Talanta* 234 (2021) 122690.